RSC Advances

This article can be cited before page numbers have been issued, to do this please use: X. hu, J. bai, J. wang, C. li and W. xu, *RSC Adv.*, 2014, DOI: 10.1039/C4RA14783A.

ROYAL SOCIETY
OF CHEMISTRY

www.rsc.org/advances

View Article Online
DOI: 10.1039/C4RA14783A

Preparation of 4A-zeolite base Ag nanoparticles composite catalyst and research of the catalytic properties

Xiaosong Hu, Jie Bai*, Junzhong Wang, Chunping Li, Wei Xu

Chemical Engineering College, Inner Mongolia University of Technology, Huhhote, 010051, People's Republic of China

*Corresponding authors: Jie Bai

Tel: +86471 6575722.

Fax: +86471 6575722.

E-mail address: baijie@imut.edu.cn

View Article Online
DOI: 10.1039/C4RA14783A

Abstract:

4A-zeolite base silver nanoparticles (Ag NPs) composite catalyst was prepared and the catalytic properties were researched. The coal gangue as raw materials, hydrothermal method was used to synthesis 4A-zeolite. Ag NPs were prepared by situ reduction method. The 4A-zeolite base Ag NPs composite catalyst was prepared by impregnation method. The catalyst was analyzed by a series of characterization techniques such as scanning electron microscopy (SEM), transmission electron microscopy (TEM), UV-Visible spectroscopy (UV-Vis), X-ray diffraction (XRD), X-ray photoelectron spectroscopy (XPS), etc. The characterization results indicated that the Ag NPs were uniformly distributed on the 4A-zeolite. Then, the catalyst was used to catalyze the epoxidation of styrene. The oxidant was tert-butyl hydroperoxide (TBHP), and Isopropanol was used as the solvent. The good catalytic properties of the composite catalyst were showed to us. The results showed very high conversion of styrene (72.1%) and excellent styrene oxide (SO) selectivity (59.5%). What’s more, the joint selectivity of SO and benzaldehyde (BZ) reached 93.3%.

Keywords: 4A-zeolite; Ag Nanoparticles; Composite catalyst; Styrene; Epoxidation

View Article Online
DOI: 10.1039/C4RA14783A

1. Introduction

4A-zeolite has a good adsorption performance and ion exchange properties [1-3], it is widely used in petrochemical industry and environmental protection and other fields in recent years [4].

Silver catalyst showed a good catalytic activity on the oxidation reaction, and its large-scale application is limited because the price of silver is more expensive. The development of nanotechnology makes its application possible. Physical properties and chemical properties of nano-silver are relatively stable, and the electronic and catalytic performance of nano-silver is very excellent. The application prospect is broad in the battery electrode material, catalyst materials, medical materials, etc [5-7].

Preparation methods of nano-silver have both physical method and chemical method. Physical methods mainly include method of laser ablation of metal [8−11] and metal vapor deposition method [12, 13]. Chemical methods include gas phase reduction method, liquid phase reduction method and solid phase reduction method [14-17]. Liquid phase reduction method has been widely applied because of its low cost, simple operation, and low requirements for equipment. The size and shape of the nanoparticles as well as the morphology of particles aggregation were effectively controlled by controlling the proportion of reducing agent and protective agent.

It will improve the specific surface area of nanoparticles and its catalytic performance that nano-silver is loaded to the 4A-zeolite, and it can be used to catalyze oxidation reaction as a high efficient catalyst [18-20]. In addition, the combination of the two substances promotes the recycling of catalyst, and the preparation cost of catalyst

View Article Online
DOI: 10.1039/C4RA14783A

will decrease, too.

Epoxides are important intermediates for the manufacture of a range of modern commercial products such as epoxy resins, textiles, surface coatings, and biological chemicals [21]. Styrene oxide and benzaldehyde are the important intermediate of medicine and spice. In addition, benzaldehyde is the important chemical raw materials. In recent years, more and more researchers pay their attention to styrene epoxidation [22-27].

First of all, coal gangue synthesis of 4A-zeolite was used, and Ag NPs were prepared by using in situ reduction method in this experiment. Then, the two substances were mixed and nano-silver would be loaded to the 4A-zeolite. The 4A-zeolite base Ag NPs composite catalyst was used to catalyze epoxidation reaction of styrene (Fig. 1), benzaldehyde, styrene oxide, and others were obtained [28-32].

View Article Online
DOI: 10.1039/C4RA14783A

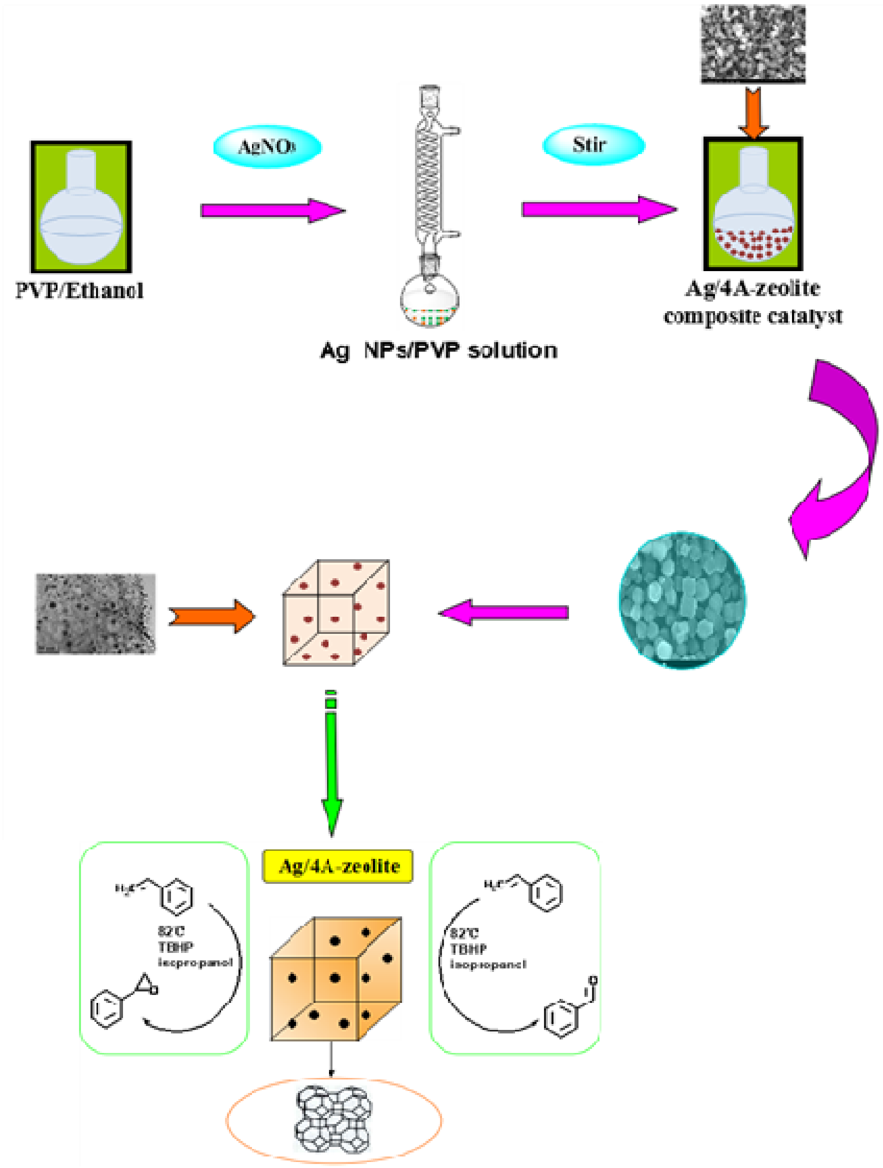

Fig. 1 Scheme of preparing the Ag NPs/4A-zeolite composite catalyst and chemical equation of styrene epoxidation.

2. Experimental

2.1.Materials

Sodium hydroxide (NaOH, AR), polyvinylpyrrolidone (PVP, Mw=10000, AR) and absolute ethyl alcohol (C_2H_5OH, AR) were purchased from China Medicine Group. Deionized water was prepared by our university. Silver nitrate ($AgNO_3$, AR,

DOI: 10.1039/C4RA14783A

99.8%) was provided by Tianjin Yingda Sparseness & Noble Reagent Chemical Factory. Styrene (C_8H_8, AR, 99.0%) was purchased from Sinopharm Chemical Reagent Co. Ltd. Isopropanol ($(CH_3)_2CHOH$, AR, 99.5%) was purchased from Tianjin Beichen Founder Reagent Plant. Tert-Butyl hydroperoxide ($(CH_3)_3COOH$, AR, 70%) was purchased from Tianjin Alfa Aesar Chemical Co. Ltd. All the chemicals were used as received without further purification.

2.2. Preparation of 4A-zeolite

Coal gangue powder was got by coal gangue crushing and sieving through 200 mesh sieve, then the activated coal gangue powder was available by calcining the coal gangue powder for 1 h under 720 ℃. The activated coal gangue powder, Sodium hydroxide and deionized water were mixed by certain proportion, and the mixture was stirred for 1h under 25 ℃. The mixture was transferred to the hydrothermal reaction kettle after the stirring was over. The hydrothermal reaction kettle was put into the vacuum drying oven, and the kettle was maintained 6.5 h under 100 ℃. Finally, the 4A-zeolite would be got after the suction filtration and drying. The pH needed to be controlled at 8 or so in the process of the suction filtration.

2.3. Preparation of silver nanoparticles

First of all, a certain amount of PVP (1.3040 g) and anhydrous ethanol (25 ml) were mixed for 12 h at 25 ℃, and PVP would be fully dissolved in anhydrous ethanol. Then a certain amount of silver nitrate was put into the mixed solution, and the proportion of silver nitrate with PVP was 1:10. Mixed solution was heated for 20 minutes through the circulating water backflow under the condition of 80 ℃. It was

View Article Online
DOI: 10.1039/C4RA14783A

important to note the seal in the process of experiment.

2.4. Preparation of 4A-zeolite base Ag NPs composite catalyst and Catalytic performance

The 4A-zeolite (1 g) which had been prepared was put into the solution containing the Ag NPs. Then the solution was stirred for 24 h at room temperature, and the 4A-zeolite base Ag NPs composite catalyst would be got after the process of suction filtration and drying. The 4A-zeolite should be activated for 2 h in 400 ℃ before it was put into the solution containing the Ag NPs.

The styrene epoxidation was carried at atmospheric pressure. The reaction mixture which contained 1 ml styrene, 5 ml TBHP, 5 ml Isopropanol and a certain account of catalyst (0.1 g-0.5 g) was put into a 25 ml round bottom flask. Then, the reaction would take place under reflux (at 82 ℃) and sufficient stirring for a period of time (12 h-48 h). The composite catalyst of Ag NPs/4A-zeolite was used in the styrene epoxidation. The catalyst was separated from the reaction mixture by filtration. The reaction products and unconverted reactants were analyzed by an Agilent (7890A) gas chromatograph (GC) and Agilent (5975C) gas chromatography mass spectrometer (GC-MS). The GC was equipped with a flame ionization detector (FID) which contained capillary column (SE-30) and N_2 as carrier gas. By an area normalization method, the conversion of styrene and the content of each component in the products were calculated. The styrene conversion and product selectivity were calculated as follows:

Styrene conversion (%) = [(areas of reactant converted) × 100] / [areas of reactant

View Article Online
DOI: 10.1039/C4RA14783A

used]

Product selectivity (%) = [(areas of product formed) × 100] / [areas of reactant converted]

2.5. Characterization of catalyst

The samples were investigated by a scanning electron microscope (SEM, Hitachi, S-3400N, Japan) which was equipped with an energy dispersive spectrometer (EDS) and transmission electron microscope (TEM, Jeol, JEM-2010, Japan and Fei, F20S-TWIN, Tecnai). The samples for TEM were dispersed in ethanol by ultrasonic treatment; and a drop of the dispersion was deposited on a TEM carbon-coated Cu grid and dried at room temperature. The UV absorbance of the obtained Ag/4A-zeolite was measured by SHIMADZU, UV-3600 UV–Vis recording spectrophotometer (Japan) with a variable wavelength between 200 and 600 nm, which was applied to detect UV absorbance of a solid sample. The UV absorbance of liquid sample was measured by SHIMADZU, UV3150 UV–visible spectrophotometer with a variable wavelength between 200 and 600 nm using 10 mm quartz cells. The phase and crystalline structures of 4A-zeolite and Ag NPs were characterized by an X-ray diffractometer (XRD, PIGAKV, D/MAX-2500/PC, Japan) over a range of 2θ angles from 5°to 80°. The measurements of the X-ray photoelectron spectroscopy (XPS) were performed by using a Thermo fisher Scientific ESCALAB 250 spectrometer.

3. Results and discussions

3.1.Characterization of catalysts

View Article Online
DOI: 10.1039/C4RA14783A

3.1.1. Scanning electron micrograph study

Fig. 2 was the SEM images of 4A-zeolite (Fig. 2A) and Ag NPs/4A-zeolite composite catalyst (Fig. 2B). From the Fig. 2A, it was shown that 4A-zeolite had the cube structure and the size of 4A-zeolite was different from 1μm to 1.5 μm. The images indicated smooth surface and uniform diameter 4A-zeolite had been prepared successfully. In addition, the aggregation phenomenon of zeolite wasn't seen in Fig. 2A and Fig. 2B. The zeolite had explicit shape on the border. It was shown that the 4A-zeolite had a rather good dispersion. After compared with Fig. 2A and Fig. 2B, it was found that the morphology of zeolite had no changed. It indicated that the addition of Ag NPs didn't affect the structure of 4A-zeolite, which attributed to the relatively stable of zeolite frame. Ag NPs/4A-zeolite composite catalyst was performed on EDS equipped in the SEM. The EDS analysis revealed that the obtained Ag NPs/ 4A-zeolite composite catalyst contained Si, Al, O, Na and Ag elements. It had been shown that silver had been loaded to the zeolite through the analysis of Fig. 2C.

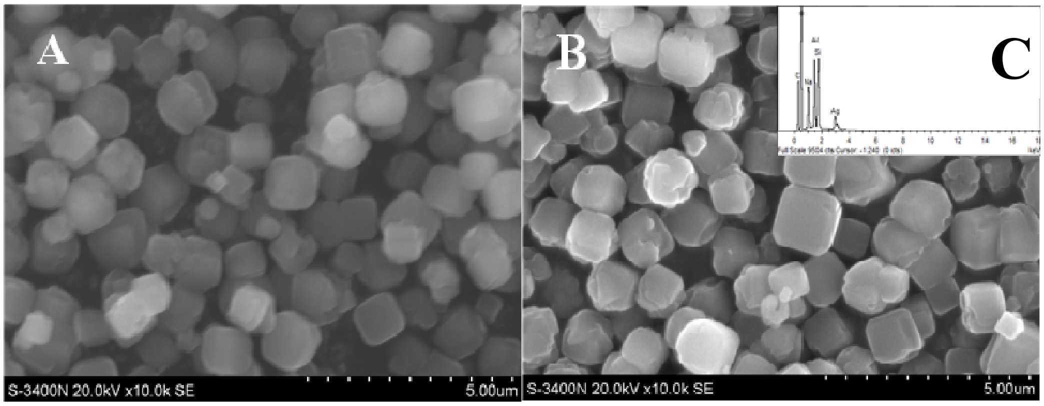

Fig. 2 SEM images of the 4A-zeolite (A) and Ag NPs/4A-zeolite composite catalyst (B); EDS spectra of Ag NPs/4A-zeolite composite catalyst (C).

View Article Online
DOI: 10.1039/C4RA14783A

3.1.2. Powder X-ray diffraction study

The low angle powder XRD patterns of 4A-zeolite (Fig. 3A) and Ag NPs/4A-zeolite composite catalyst (Fig. 3B) were showed in Fig. 3. All the absorption peaks were detected between 5° and 80°. The absorption peaks of 4A-zeolite appeared at $2\theta = 7.2°$, 10.2°, 12.5°, 16.1°, 21.7°, 24.0°, 27.2°, 29.9° and 34.2° (JCPDS 39-0223). From Fig. 3A, it was shown that the pattern had got all the characterized absorption peak of 4A-zeolite. It was also showed that the 4A-zeolite had got higher crystallinity. After compared with Fig. 3A and Fig. 3B, the peaks were around $2\theta =$ 38.1°, 44.3° and 64.5° which were assigned to the Ag (111), (200) and (220) crystal planes, respectively. These peaks correspond to the cubic crystal structure of silver (JCPDS 04-0783). The measured spacing of crystal lattice was 0.21 nm, 0.24 nm and 0.145 nm correspond to the Ag (111), (200) and (220) crystal planes, respectively. No other characteristic peaks of impurities were observed. It indicated that the metallic Ag was found to be the only species in the catalysts. The diffraction peaks of Ag species were found relatively small, which indicated the high dispersion of Ag species on the 4A-zeolite. The results indicated that impregnation method could effectively load Ag onto the 4A-zeolite, and the silver crystalline phase was formed in the zeolite framework.

View Article Online
DOI: 10.1039/C4RA14783A

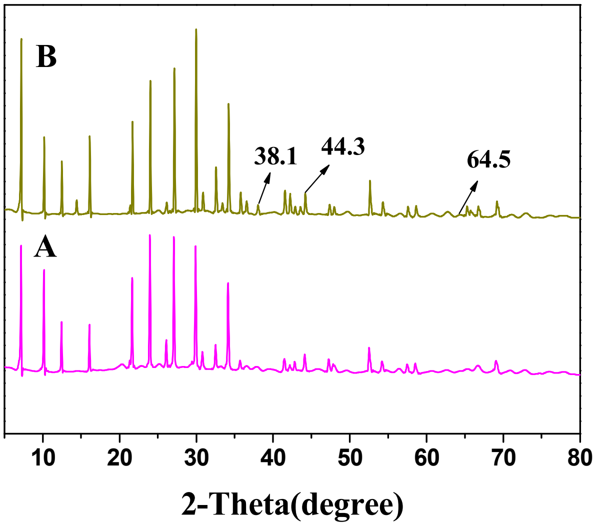

Fig. 3 XRD patterns of the 4A-zeolite (A); Ag NPs/4A-zeolite composite catalyst (B).

3.1.3. UV-Vis spectral study

The UV-Vis spectra of Ag NPs/4A-zeolite composite catalyst (Fig. 4A) and filtrate (Fig. 4B) (the liquid which was acquired in the process of preparing 4A-zeolite base Ag NPs composite catalyst) was showed in Fig. 4. From the Fig. 4A, it can be seen that a broad and characteristic absorption band associated with the formation of silver nanoparticles (Ag NPs) appeared at 383 nm, attributed to the existence of Ag NPs. In addition, a rather good dispersion of Ag NPs which was formed on the 4A-zeolite surface was found. We attained the conclusion from the high symmetry of peak. What's more, the diameters of Ag NPs were relatively small. As shown in Fig. 4B, obvious absorption band at 413 nm attributed to the Ag NPs. After compared Fig. 4B with Fig. 4A, it was shown that the peak position moved to the long wavelength, and the reasonable explanation was the gather of silver particles in the filtrate. It was

View Article Online
DOI: 10.1039/C4RA14783A

inferred from the UV-Vis spectra that the existence of Ag NPs on the zeolite.

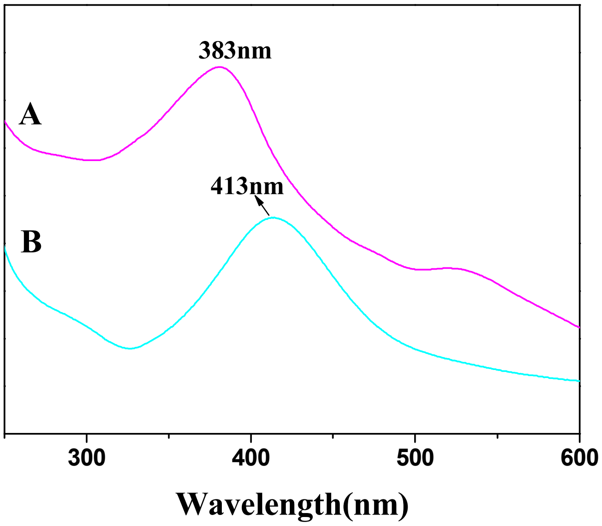

Fig. 4 Solid-UV spectra pattern of the Ag NPs/4A-zeolite composite catalyst (A) and liquid-UV spectra pattern of the filtrate (B).

3.1.4. Transmission electron micrograph study

The morphology and size of nano-silver were detected and analyzed by TEM. The TEM of Ag NPs/4A-zeolite composite catalyst was showed in Fig. 5. It was obvious that the structure of 4A-zeolite had no change. It was clearly observed that there were a large number of small dark spots on the surface of zeolite, which were the Ag NPs on the surface of 4A-zeolite. The surface of the 4A-zeolite was covered with Ag NPs, and the Ag particles were distributed very uniformly. In addition, the aggregation phenomenon of particles wasn't seen in Fig. 5A, Fig. 5B and Fig. 5C, because of the addition of protective agent (PVP) when the Ag NPs were prepared. In Fig. 5D, it was the HRTEM image of the Ag NPs/4A-zeolite composite catalyst. The crystal lattice was seen clearly in the surface of the Ag NPs/4A-zeolite composite

View Article Online
DOI: 10.1039/C4RA14783A

catalyst, and the measured spacing was 0.21 nm, corresponding to the interplanar (200) spacing of Ag NPs, as observed by the above XRD patterns. Thus, it could be confirmed that the Ag NPs with an average size of about 5-10 nm were uniformly distributed on the surface of 4A-zeolite.

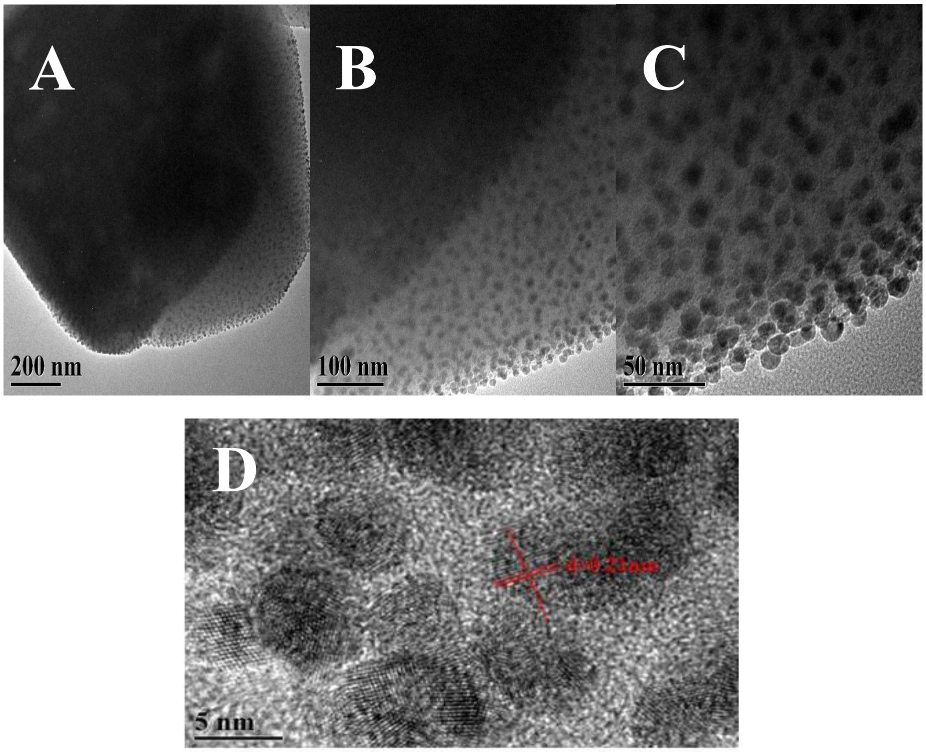

Fig. 5 TEM images of Ag NPs/4A-zeolite composite catalyst (A, B and C) and HRTEM image of Ag NPs/4A-zeolite composite catalyst (D).

3.1.5. X-ray photoelectron spectroscopy study

The characterization of XPS was performed in order to confirm the electronic states of Ag on the catalyst. Fig. 6 was the XPS patterns for the Ag NPs/4A-zeolite composite catalyst. In Fig. 6A, it was shown that the fully scanned spectra in the range of 0-1300 eV of Ag/4A-zeolite. The C, Si, Al, O, Na and Ag were demonstrated to exist in the Ag NPs/4A-zeolite composite catalyst. The Si, Al, O and Na were the

View Article Online
DOI: 10.1039/C4RA14783A

chemical elements of 4A-zeolite. In Fig. 6B, two peaks with high intensity were observed at 368.5 eV and 374.5 eV, which were assigned to the photoelectron spectra of Ag 3d. These peaks correspond well with Ag $3d_{5/2}$ and Ag $3d_{3/2}$ binding energies, respectively. It was shown that Ag^0 was the only state of Ag existed in the composite catalyst. The conclusion was that the Ag^0 had been loaded onto the 4A-zeolite. It indicated that Ag^0 was the only active component which promoted the styrene epoxidation on the surface of 4A-zeolite.

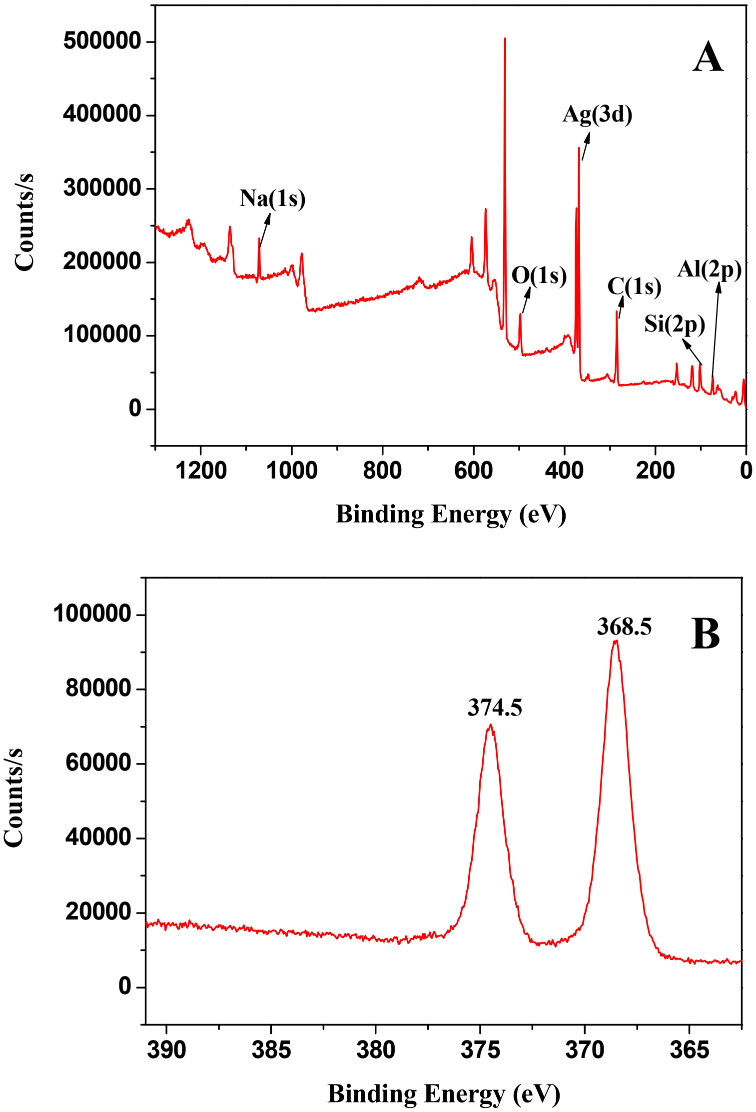

View Article Online
DOI: 10.1039/C4RA14783A

Fig. 6 XPS pattern of the Ag NPs/4A-zeolite composite catalyst.

3.2. Catalytic activity

Many solid catalysts reported in the literatures showed high product selectivity with TBHP as the oxidant [22, 23, 25, 33]. Thus, in this work, the catalytic activities of Ag NPs/4A-zeolite composite catalyst were tested in the epoxidation of styrene with TBHP as the oxidant. In order to get the optimal reaction conditions, different parameters such as catalyst amount and reaction time were investigated. After the analysis of GC and GC-MS detection, the main products of the reaction were styrene oxide (SO) and benzaldehyde (BZ).

The influence of catalyst amount on the catalytic performance was investigated by varying the catalyst amount from 0.1 g to 0.5 g and the consequences were shown in Table 1. The reaction time was 24 h and the temperature was kept in 82 ℃. From the table, it was found that the highest conversion of styrene (55.1%) appeared when 0.1 g catalyst was used. The conversion of styrene had no improvement with the increase of the catalyst amount, but the selectivity of styrene oxide and benzaldehyde increased slightly. It is worth noting that the selectivity of styrene oxide and benzaldehyde decreased obviously under 0.5 g catalyst. The optimal catalyst amount was 0.1 g by the comprehensive consideration. So we chose this value to continue the examination of reaction time.

It was investigated that the reaction time effected on the catalytic performance after added 0.1 g catalyst into the catalytic reaction, and the consequences were showed in Table 2. The reaction temperature was kept in 82 ℃. From the table, it was shown that the reaction time had obvious influence on the catalytic performance. The conversion of styrene and the styrene oxide selectivity had got obvious improvement with the increase of the reaction time. The highest selectivity of styrene oxide appeared at 48 h. However, the conversion of styrene increased slowly while the selectivity of styrene oxide and benzaldehyde decreased obviously from 48 h to 60 h. It indicated that the styrene oxide and benzaldehyde started to turn into other by-products. Therefore, further prolonging reaction time made no sense on the styrene epoxidation after 48 h. There is no doubt that the reaction time played a key role in styrene epoxidation reaction. The results showed that the optimal reaction time was 48 h. The conversion of styrene was 72.1% and the selectivity of styrene oxide was 59.5%. The yield of styrene oxide was 42.9%. What’s more, the joint selectivity of styrene oxide and benzaldehyde reached 93.3%.

In addition, the catalytic performance of 4A-zeolite and blank control group were investigated under the 24 h. The catalytic results of 4A-zeolite, Ag/4A-zeolite and blank control were shown in Table 3. Compared with the blank, 4A-zeolite slightly improved the conversion of styrene and selectivity of styrene oxide. It was shown that the conversion of styrene increased slightly while the selectivity of styrene oxide increased obviously from 18.2% to 50.4% when Ag NPs were added to the 4A-zeolite. What’s more, the selectivity of benzaldehyde and other by-products decreased obviously. The yield of styrene oxide increased from 9.7% to 27.8%. So the Ag NPs/4A-zeolite composite catalyst showed sufficient capacity on styrene epoxidation.

View Article Online
DOI: 10.1039/C4RA14783A

Table 1 Epoxidation of styrene under various catalyst dosages

Entry	*Catalyst (g)*	*Time (h)*	*Conversion (%)*	*Selectivity (%)*		
				SO	BZ	Others
1	0.1	24	55.1	50.4	32.8	16.8
2	0.2	24	53.2	56.1	35.7	8.2
3	0.3	24	53.9	59.0	33.2	7.8
4	0.4	24	53.0	58.1	35.6	6.3
5	0.5	24	53.3	53.0	27.7	19.3

Table 2 Epoxidation of styrene under various reaction times

Entry	*Catalyst (g)*	*Time (h)*	*Conversion (%)*	*Selectivity (%)*		
				SO	BZ	Others
1	0.1	12	35.9	45.5	40.4	14.1
2	0.1	24	55.1	50.4	32.8	16.8
3	0.1	36	66.4	56.4	30.3	13.3
4	0.1	48	72.1	59.5	33.8	6.7
5	0.1	60	77.8	45.9	28.7	25.3

Table 3 Comparison of Ag/4A-zeolite catalyst with the 4A-zeolite and blank control for the styrene epoxidation reaction

Entry	*Catalyst*	*Time (h)*	*Conversion (%)*	*Selectivity (%)*		
				SO	BZ	Others
1	-	24	51.9	16.3	46.2	37.5
2	4A-zeolite (0.1g)	24	53.1	18.2	46.4	35.4
3	Ag/4A-zeolite (0.1g)	24	55.1	50.4	32.8	16.8

4. Conclusions

A kind of composite catalyst involving silver NPs supported on a 4A-zeolite was prepared. The catalyst was characterized by SEM, XRD, UV, TEM and XPS. After the analysis of all the characterization, the results showed that the 4A-zeolite morphology and crystallinity was better, and the silver NPs was proved to load onto the 4A-zeolite and evenly distributed. It was shown that the diameter of silver NPs was from 5 to 15 nm according to the figure of particle size distribution. Then the composite catalyst was used to the epoxidation of styrene with TBHP as oxidant. The different parameters such as catalyst amount and reaction time were investigated. The optimal catalyst amount was 0.1 g and the optimal reaction time was 48 h. The Ag NPs/4A-zeolite composite catalyst showed good catalytic activity for the epoxidation of styrene. The conversion of styrene was 72.1% and the selectivity of SO was 59.5%. In addition, the joint selectivity of SO and BZ was 93.3%. We could conclude that the Ag^0 which was added to the 4A-zeolite promoted the epoxidation of styrene. It would improve the specific surface area of nanoparticles and increase the contact area between Ag NPs and reactant that Ag NPs were added to 4A-zeolite support. What’s more, the catalytic performance would be improved when Ag NPs were distributed very uniformly on the surface of 4A-zeolite. The highly dispersive Ag NPs significantly improve the yield of styrene oxide.

View Article Online
DOI: 10.1039/C4RA14783A

REFERENCES

[1] A. Mayoral, T. Carey, P. A. Anderson, *Microporous and Mesoporous Materials*, 2012, 166, 117-122.

[2] D. H. Kim, J. Kim, *Journal of Phsics and Chemistry of Solids*, 2007, 68, 734.

[3] C. W. Kim, J. S. Park, K. S. Lee, *Power Sources*, 2006, 163, 144.

[4] Bibby, M. P. Dale, *Nature*, 1985 (317), 157-158.

[5] G. G. Lenzi, C. V. B. Favero, *Desalination*, 2011, 270 (1-3), 241-247.

[6] H. Shiomi, H. Furukawa, *Journal of Materials Science-Materials in Electronics*, 2000, 11 (1), 7-31.

[7] M. D. Morris, *Spie-int Soc Optical Engineering*, 1999, 224-229.

[8] S. Yang, W. Cai, G. Liu, *Journal of Physical Chemistry C*, 2009, 113 (16), 6480-6484.

[9] H. Muto, K. Yamada, K. Miyajima and F. Mafune, *Journal of Physical Chemistry C*, 2007, 111 (46), 17221-17226.

[10] P. Liu, W. Cai and H. Zeng, *Journal of Physical Chemistry C*, 2008, 112 (9), 3261-3266.

[11] S. Hashimoto, T. Uwada, H. Masuhara and T. Asahi, *Journal of Physical Chemistry C*, 2008, 112 (39), 15089-15093.

[12] K. Wegner, B. Walker, S. Tsantilis and S. E. Pratsinis, *Chemical Engineering Science*, 2002, 57 (10), 1753-1762.

[13] C. C. Chen, C. C. Yeh, *Advanced Materials*, 2000, 12 (10), 738-741.

View Article Online
DOI: 10.1039/C4RA14783A

[14] Z. S. Pillai, P. V. Kamat, *Journal of Physical Chemistry B*, 2004, 108 (3), 945-951.

[15] Y. Sun, B. Mayers, T. Herricks, *Nano Letters*, 2003, 3 (7), 955-960.

[16] D. H. Chen, Y. W. Huang, *Journal of colloid and interface science*, 2002, 255 (2), 299-302.

[17] H. J. Jiang, K. S. Moon1, Z. Q. Zhang, *Journal of Nanoparticle Research*, 2006, 8, 117-124.

[18] C. Zakri, P. Poulin, *Nano Letters*, 2005, 5 (11), 2212-2215.

[19] K. A. Bethke, H. H. Kung, *Journal of Catalysis*, 1997, 172 (1), 93-102.

[20] Li. Z, Flytzani. S. M, *Journal of Catalysis*, 1999, 182 (2), 313-327.

[21] H. Nakajima, S. Takase, H. Terano and H. Tanaka, *Journal of Antibiotics*, 1997, 50, 96-99.

[22] H. Liu, J. Bai, C. P. Li, W. Xu, W. Y. Sun, T. Xu, Y. R. Huang and H. Q. Li, *RSC Advances*, 2014, 4, 3195-3200.

[23] B. Singh, A. K. Sinha, *Journal of Materials Chemistry A*, 2014, 2, 1930-1939.

[24] Z. Q. Shi, L. X. Jiao, J. Sun, Z. B. Chen, Y. Z. Chen, X. H. Zhu, J. H. Zhou, X. C. Zhou, X. Z. Li and R. Li, *RSC Advances*, 2014, 4, 47-53.

[25] H. Liu, J. Bai, S. Wang, C. P. Li, L. P. Guo, H. O. Liang, T. Xu, W. Y. Sun and H. Q. Li, *Colloids and Surfaces A*, 2014, 448, 154-159.

[26] H. Lin, Y. Liu and Z. L. Wu, *Chemical Communications*, 2011, 47, 2610-2612.

[27] L. Zhou, C. F. Gorin and R. J. Madix, *Journal of the American Chemical Society*, 2010, 132, 434-435.

View Article Online
DOI: 10.1039/C4RA14783A

[28] M. Silva, C. Freire, B. De Castro, J. L. Figueiredo, *Journal of Molecular Catalysis A*, 2006, 258, 327-333.

[29] X. T. Wang, Z. Q. Liang, F. Z. Zhang, L. Yang and S. L. Xu, *Journal of Materials Science*, 2013, 48, 5899-5903.

[30] J. Sun, Q. B. Kan, Z. F. Li, G. L. Yu, H. Liu, X. Y. Yang, Q. S. Huo and J. Q. Guan, *RSC Advances*, 2013, 4, 2310-2317.

[31] M. M. Hussain and P. J. Walsh, *Accounts of Chemical Research*, 2008, 41, 883–893.

[32] D. S. Pinnaduwage, L. Zhou, W. W. Gao and C. M. Friend, *Journal of the American Chemical Society*, 2007, 129, 1872–1873.

[33] J. H. Liu, F. Wang, S. S. Qi, Z. G. Gu and G. D. Wu, *New Journal of Chemistry*, 2013, 37, 769–774.

View Article Online
DOI: 10.1039/C4RA14783A

Figure Captions:

Fig. 1 Scheme of preparing the Ag NPs/4A-zeolite composite catalyst and chemical equation of styrene epoxidation.

Fig. 2 SEM images of the 4A-zeolite (A) and Ag NPs/4A-zeolite composite catalyst (B); EDS spectra of Ag NPs/4A-zeolite composite catalyst (C).

Fig. 3 XRD patterns of the 4A-zeolite (A); Ag NPs/4A-zeolite composite catalyst (B).

Fig. 4 Solid-UV spectra pattern of the Ag NPs/4A-zeolite composite catalyst (A) and liquid-UV spectra pattern of the filtrate (B).

Fig. 5 TEM images of Ag NPs/4A-zeolite composite catalyst (A and B) and HRTEM image of Ag NPs/4A-zeolite composite catalyst (C).

Fig. 6 XPS pattern of the Ag NPs/4A-zeolite composite catalyst.

Table 1 Epoxidation of styrene under various catalyst dosages.

Table 2 Epoxidation of styrene under various reaction times.

Table 3 Comparison of Ag/4A-zeolite catalyst with the 4A-zeolite and blank control for the styrene epoxidation reaction.

View Article Online
DOI: 10.1039/C4RA14783A

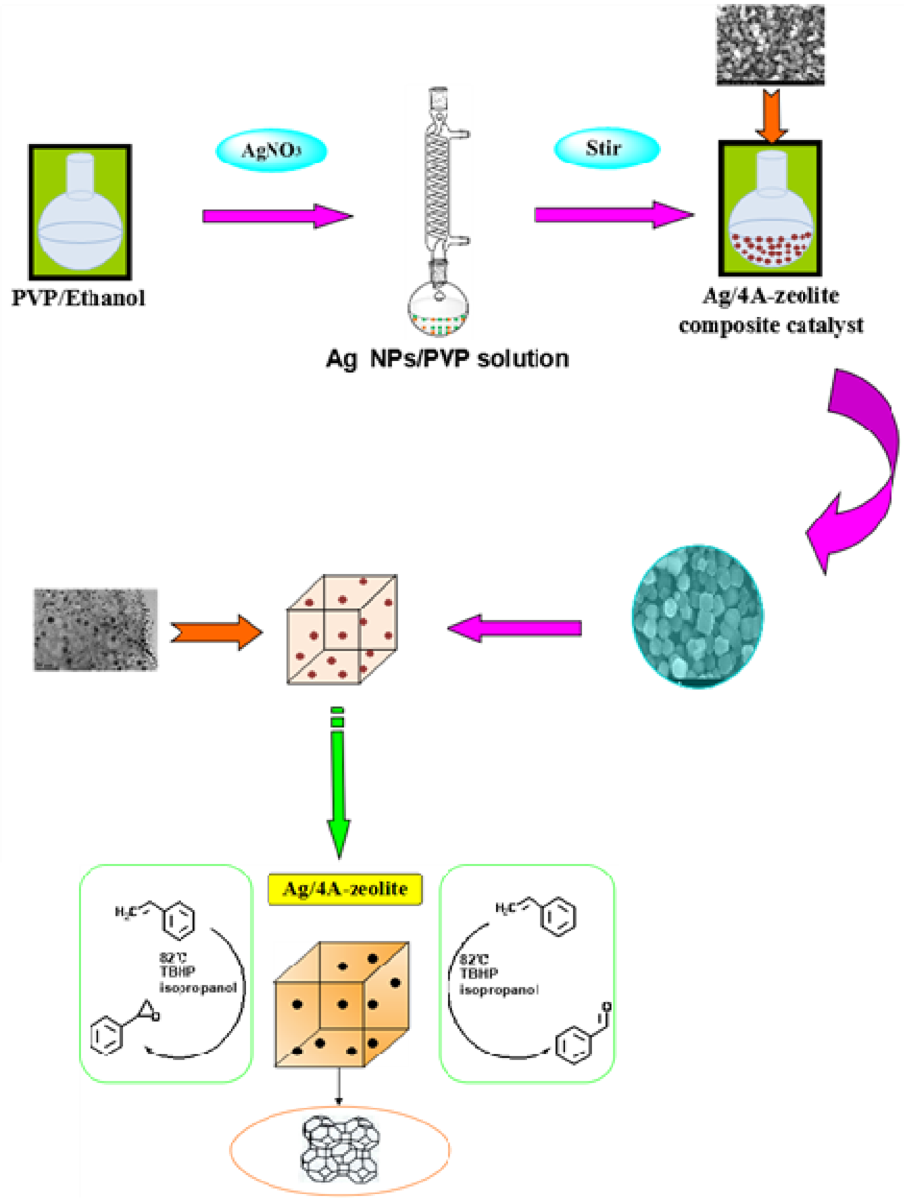

Fig. 1

View Article Online
DOI: 10.1039/C4RA14783A

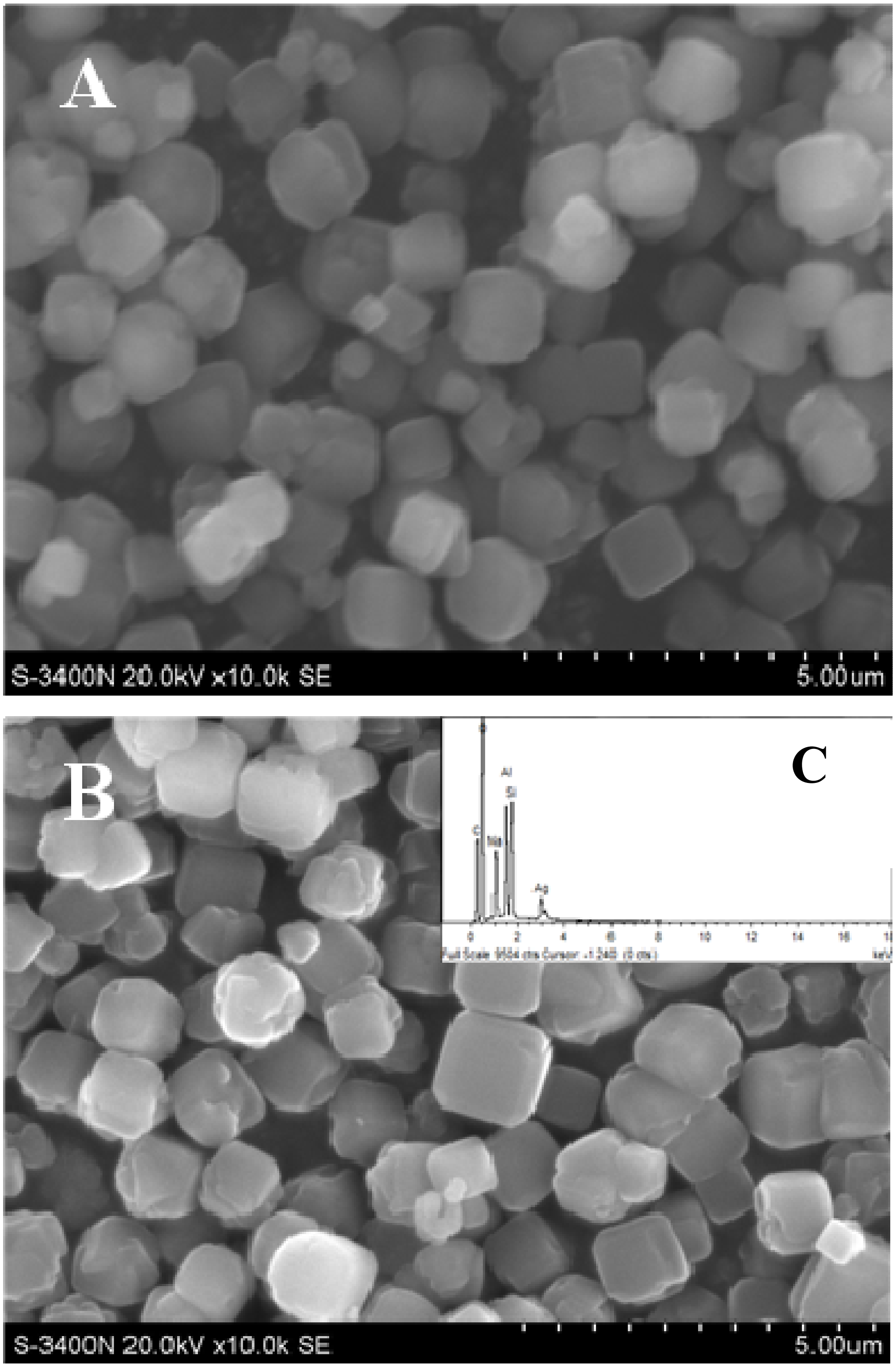

Fig. 2

View Article Online
DOI: 10.1039/C4RA14783A

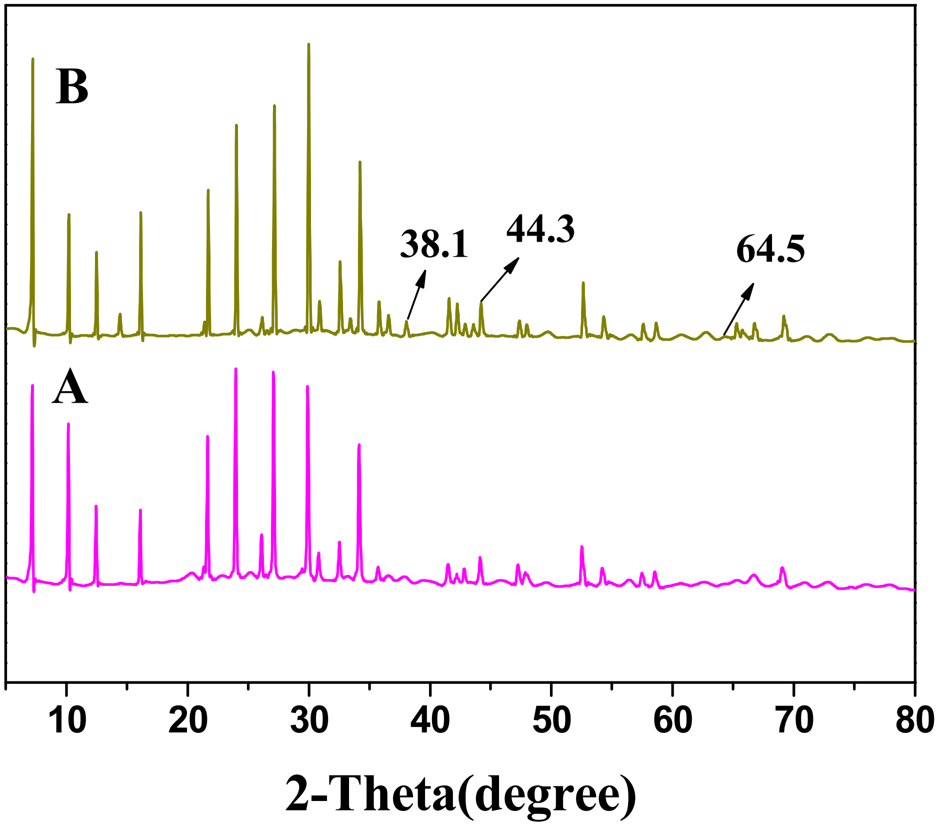

Fig. 3

View Article Online
DOI: 10.1039/C4RA14783A

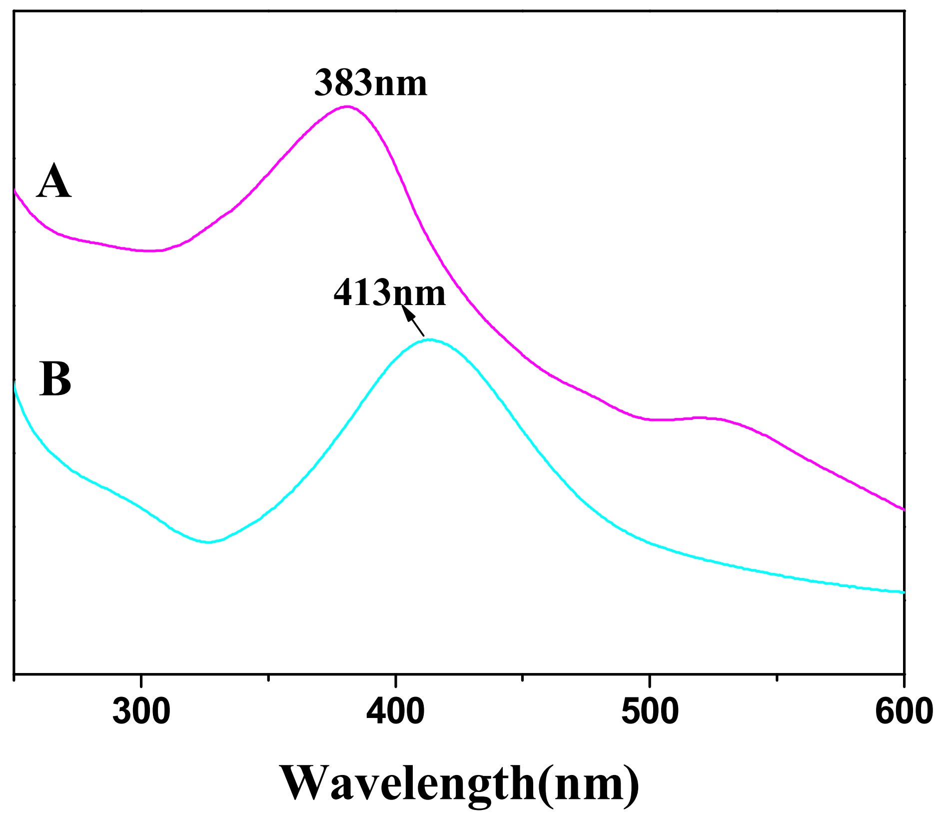

Fig. 4

View Article Online
DOI: 10.1039/C4RA14783A

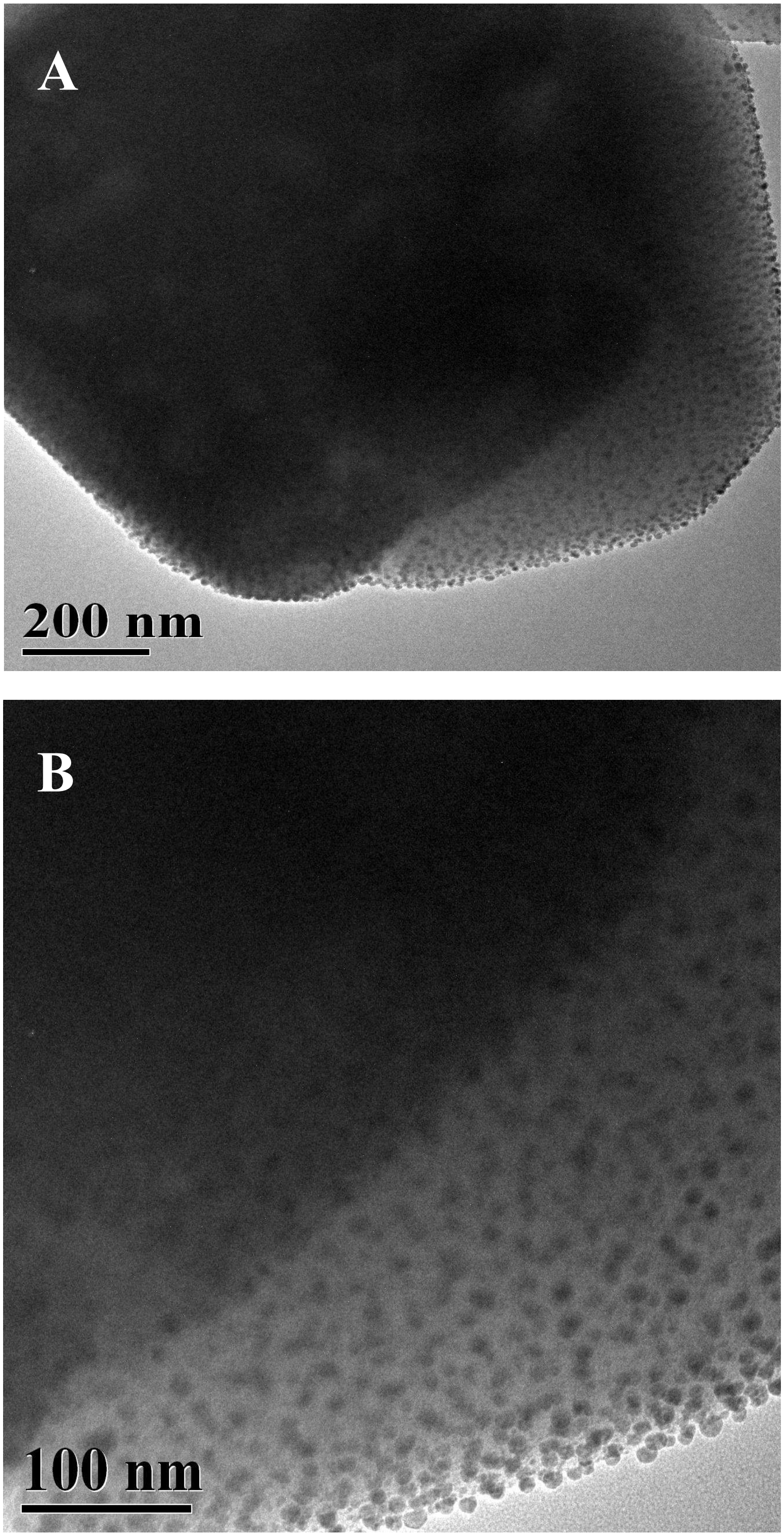

View Article Online
DOI: 10.1039/C4RA14783A

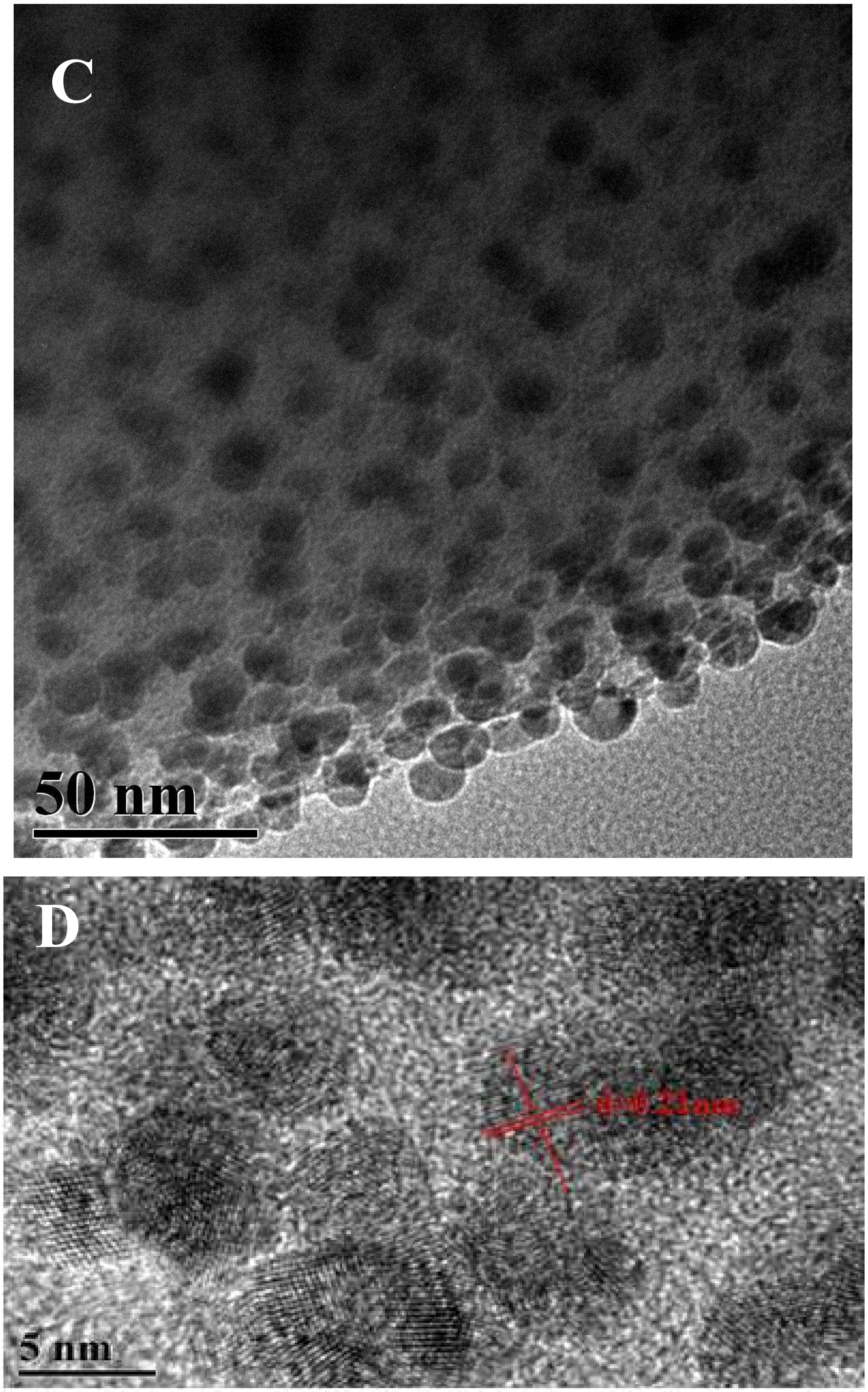

Fig. 5

DOI: 10.1039/C4RA14783A

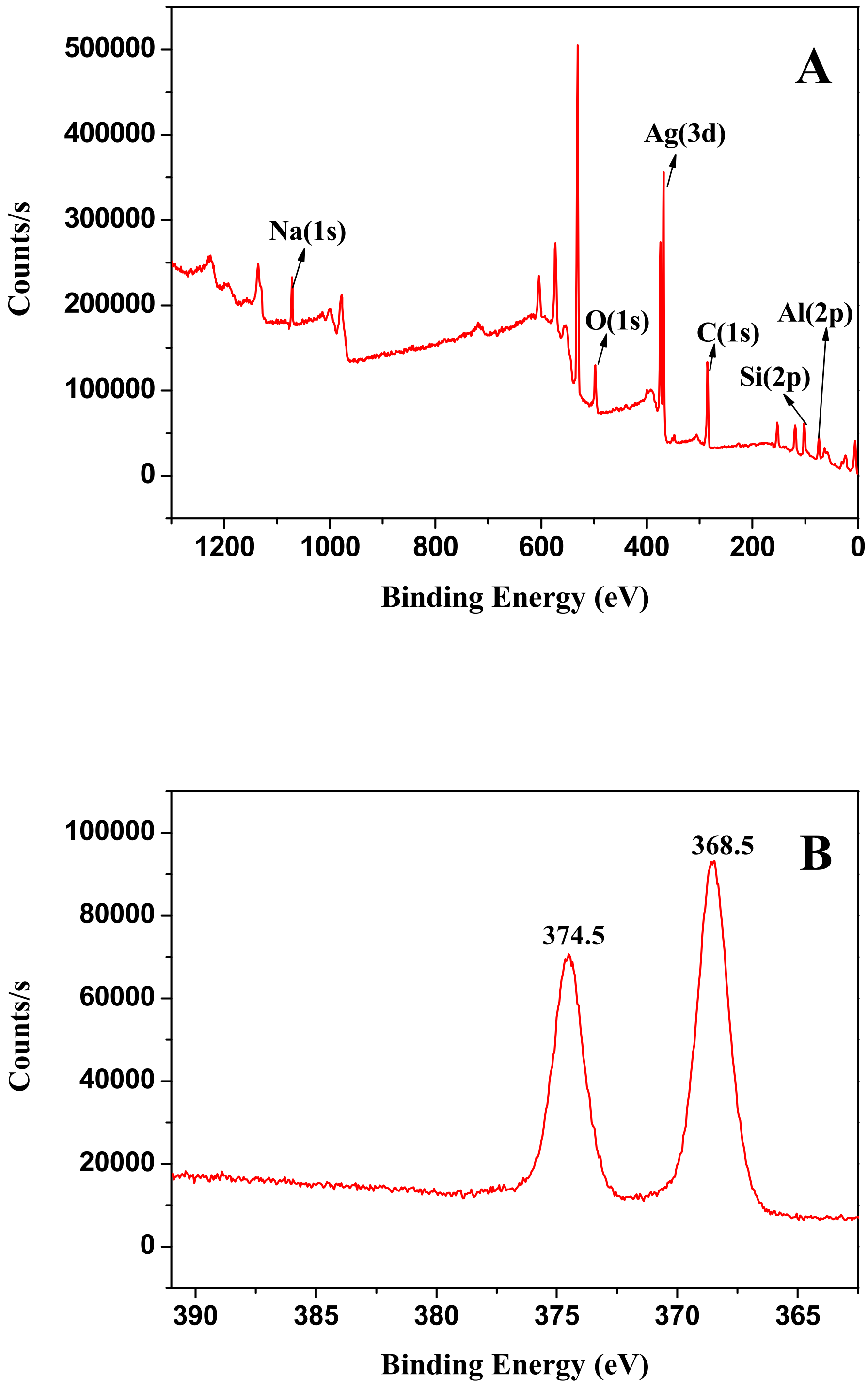

Fig. 6

View Article Online
DOI: 10.1039/C4RA14783A

Table 1

Entry	*Catalyst (g)*	*Time (h)*	*Conversion (%)*	*Selectivity (%)*		
				SO	BZ	Others
1	0.1	24	55.1	53.4	34.7	16.8
2	0.2	24	53.2	56.1	35.7	8.2
3	0.3	24	53.9	59.0	33.2	7.8
4	0.4	24	53.0	58.1	35.6	6.3
5	0.5	24	53.3	53.0	27.7	19.3

Table 2

Entry	*Catalyst (g)*	*Time (h)*	*Conversion (%)*	*Selectivity (%)*		
				SO	BZ	Others
1	0.1	12	35.9	45.5	40.4	14.1
2	0.1	24	55.1	50.4	32.8	16.8
3	0.1	36	66.4	56.4	30.3	13.3
4	0.1	48	72.1	59.5	33.8	6.7
5	0.1	60	77.8	45.9	28.7	25.3

View Article Online
DOI: 10.1039/C4RA14783A

Table 3

Entry	*Catalyst*	*Time (h)*	*Conversion (%)*	*Selectivity (%)*		
				SO	**BZ**	**Others**
1	**-**	**24**	**51.9**	**16.3**	**46.2**	**37.5**
2	**4A-zeolite （0.1g）**	**24**	**53.1**	**18.2**	**46.4**	**35.4**
3	**Ag/4A-zeolite (0.1g)**	**24**	**55.1**	**50.4**	**32.8**	**16.8**